2006ESASP.624E.103J

A COMPARISON OF ACOUSTIC MODE PARAMETERS USING MULTI-SPECTRAL DATA

Kiran Jain[1], Frank Hill[1], S. C. Tripathy[1], H. M. Antia[2], J. D. Armstrong[3], S. M. Jefferies[3], E. J. Rhodes, Jr.[4], and P. J. Rose[4]

[1]*National Solar Observatory, 950 North Cherry Avenue, Tucson, AZ 85719, USA*
[2]*Tata Institute of Astrophysics, Homi Bhabha Road, Mumbai 400005, India*
[3]*Institute for Astronomy, University of Hawaii, 4761 Lower Kula Road, Kula, HI 96790, USA*
[4]*University of Southern California, 835 W. 37th Street, SHS, Los Angeles, California 90089-1341, USA*

ABSTRACT

We study the variation in characteristics of the high-degree modes such as frequency, amplitude, line width with the type of spectral line used to observe the solar oscillation. The technique used here is the ring-diagram analysis, which has been proven a powerful tool in local helioseismic studies. The data sets include simultaneous observations obtained with the Ni I 676.8 nm from GONG, K I 769.9 nm from Magneto-Optical filters at Two Heights (MOTH) experiment and Na I D_2 589.0 nm from MOTH experiment and Mount Wilson Observatory (MWO) during Austral summer of 2002-03. We use two different models to fit the power spectra obtained from the ring-diagram technique; the symmetric peak profile model and the asymmetric peak profile model. Our analysis clearly show that there is a significant variation in the mode amplitude for different spectral lines, however, mode frequencies and the line width or life-time of the modes are independent of the spectral line used to observe the oscillation.

Key words: Sun: oscillations, Sun: interior.

1. INTRODUCTION

Over the last several decades, the techniques of helioseismology have been widely used to study the properties and the dynamics of the solar interior. A large number of studies have been carried out to understand the variation in oscillation mode parameters with time or more precisely with the change in solar activity [1, 2, 3, 4]. However, most of the studies were confined to the global modes, mainly for low- and intermediate-degree (ℓ) modes using independent data sets e.g BISON and IRIS for low-ℓ, and GONG and MDI for intermediate-ℓ modes. These modes travel through deeper layers in the interior and provide little information about the near surface layers. The properties of the high-ℓ modes are important as they probe the outermost layers of the Sun where convection is most vigorous. However, the study of global high-ℓ modes is currently limited by the analysis techniques [5].

With the advances in various techniques of local helioseismology, it has been possible to infer properties of the high-ℓ modes and study the characteristics of the near surface layers (e.g.[6, 7]). These techniques mainly use the running waves in a localized area to infer properties as a function of heliographic latitude and longitude as well as depth. In the case of ring-diagram analysis, the mode parameters are obtained from a 3d power spectrum, which is calculated from a localized region of the solar surface. This region is tracked with an average rotation rate for a reasonable length of time. The observations are carried out with a chosen spectral line or observable. Therefore, properties of the modes may be altered if different types of images are used. Basu, Antia & Bogart [8] analyzed the characteristics of the modes obtained with velocity, intensity and line-depth images to study of effect of observables. They found that the frequencies obtained by fitting asymmetric peak profiles to different spectra agree reasonably well with each other, while use of symmetric profile gives significant difference between frequencies computed using intensity and velocity or line depth. Further, the asymmetry and the power in peaks are different while the lifetime of modes are independent of the type of observable.

In this work, we examine the difference in high-ℓ mode parameters, viz., frequency, amplitude, width, background power and asymmetry of the peak profile, to study their variation with observing height in solar atmosphere. Current solar atmospheric models indicate that the plasma density decreases with observing height, as a result, the mode amplitude should increase. We calculate mode parameters using the simultaneous observations of the Ni, K and the Na lines. We also compare our results with Rhodes et al. [9] where the same parameters were obtained for high-frequency global modes by fitting the peaks and ridges in Ni (Michelson Doppler Images, MDI) and Na (Mount Wilson Observatory, MWO) power spectra. The reliability of the results is tested by using two different type of models to fit the power spectra.

© European Space Agency • Provided by the NASA Astrophysics Data System

2006ESASP.624E.103J

2. DATA AND TECHNIQUE

In order to study the variation in mode parameters as a function of observing height, we use three simultaneous data sets. This provides a reliable comparison of mode parameters obtained with the different spectral lines. The data sets are from the Gloabal Oscillation Netwrok Group (GONG) [10], the Magneto-Optical filters at Two Heights (MOTH) [11] and the MWO [9]. The details of the data sets are summarized in Table 1. It should be noted that the Ni and K lines are formed in the photosphere while Na line is in the chromosphere. The formation height of these lines are approximately 200 km, 420 km and 780 km from the base of the photosphere, respectively.

Table 1. Details of the data sets used in this work

Data source	Spectral line (nm)	Cadence (sec)	Spatial resolution (pixel^2)	Solar radius (pixel)
GONG	Ni I 676.8	60	1024 × 1024	∼400.
MOTH	K I 769.9	10	512 × 512	178.4
MOTH	Na D_2 589.0	10	512 × 512	178.4
MWO	Na D_2 589.0	60	1024 × 1024	∼441.

The MOTH observations were carried out during December 2002 and January 2003 at the South Pole with a duty cycle of ∼100%. The continuous and simultaneous full-disk Doppler velocity and intensity images are available for four observing runs lasting between 36 and 107 hours for K and Na lines. The high-resolution full-disk Na velocity images from the Mt Wilson Observatory's 60-Foot Tower were also used for comparison but these observations are interupted by the night gaps and are only available for approximately eight hours a day. All these data sets can be accessed from the Solar Virtual Observatory (VSO) web page. We also use data sets from GONG, which provides continuous high-resolution velocity images with a duty cycle >90% using Ni line.

Since all three experiments have three different types of measurements and also different image geometries, some systematic errors may be reflected in the mode parameters. Therefore, prior to the analysis we have applied the following procedures to these data sets in order to minimize differences arising due to various image specifications;

- resampled the cadence of MOTH images at 60 seconds.
- reduced the resolution of GONG amd MWO images by reducing the solar radius to match with that of MOTH images. The scaling factors for the GONG and MWO images are 2.24 and 2.47, respectively.

We adopt the ring-diagram technique to calculate mode parameters[12], where 3d power spectra are obtained from the localized regions on the solar disk which are tracked with an average rotation rate at the solar surface. In practice, the ring-diagram technique is generally applied to the high-resolution images and a region of $15^o \times 15^o$ is tracked for 1664 minutes [13]. However, we follow a slightly different approach by considering a bigger patch. This is motivated by the lower-resolution images which makes it difficult to fit modes near the surface. The selection of a bigger area allows us to recover modes from the deeper layers, thus provding a sufficient number of modes to study their properties. But there is a trade-off between the size of the patch and the validity of the plane wave approximation used by the technique.

To extract mode parameters, the resulting power spectra was fitted with two different predefined models. The symmetric profile model considers that the peaks in the power spectra are Lorentzian (symmetric) and we fit a function of the form [13]

$$P(k_x, k_y, \omega) = \frac{A}{(\omega - \omega_0 + k_x U_x + k_y U_y)^2 + \Gamma^2} + \frac{b}{k^3} \quad (1)$$

where P is the oscillation power for a wave with a temporal frequency ω and the total wave number $k = k_x^2 + k_y^2$. There are six parameters to be fitted: two Doppler shifts ($k_x U_x$ and $k_y U_y$) for waves propagating in the orthogonal zonal and meridional directions, the background power b, the mode central frequency ω_0, the mode width Γ, and the amplitude A.

The second model is based on a function where the power in both sides of the peaks is not equally distributed. We fit a asymmetric function of the following form [14]. 2pt

$$P(k_x, k_y, \nu) = \frac{e^{b_1}}{k^3} + \frac{e^{b_2}}{k^4} + \frac{exp(A_0 + (k - k_0)A_1 + A_2(\frac{k_x}{k})^2 + A_3 \frac{k_x k_y}{k^2})S_x}{x^2 + 1} \quad (2)$$

where

$$x = \frac{\nu - ck^p - k_x U_x - k_y U_y}{\Gamma_0 + \Gamma_1(k - k_0)}, \quad (3)$$

$$S_x = s^2 + (1 + Sx)^2 \quad (4)$$

Here parameters are determined by fitting the spectra using a maximum likelihood approach: $\exp(A_0)$ is the amplitude of peak, ck^p is the mean frequency and Γ_0 is the half-width. The parameters S controls the asymmetry in the peaks. The asymmetry is generally an indication of the depth at which the modes are excited. The deeper a mode is excited, the more symmetric is the peak. The form of asymmetry is the same as that used by Nigam &

© European Space Agency • Provided by the NASA Astrophysics Data System

2006ESASP.624E.103J

Kosovichev [15] i.e. it has negative values for modes in the velocity spectra. Other parameters have the same meaning as in the case of the symmetric profile model.

In this study, we consider five regions of $30^o \times 30^o$ near the disk center to minimze the projection effect. These regions are centered at 30°N and 30°S at the central meridian, 30°E and 30°W at the equator, and the disk center.

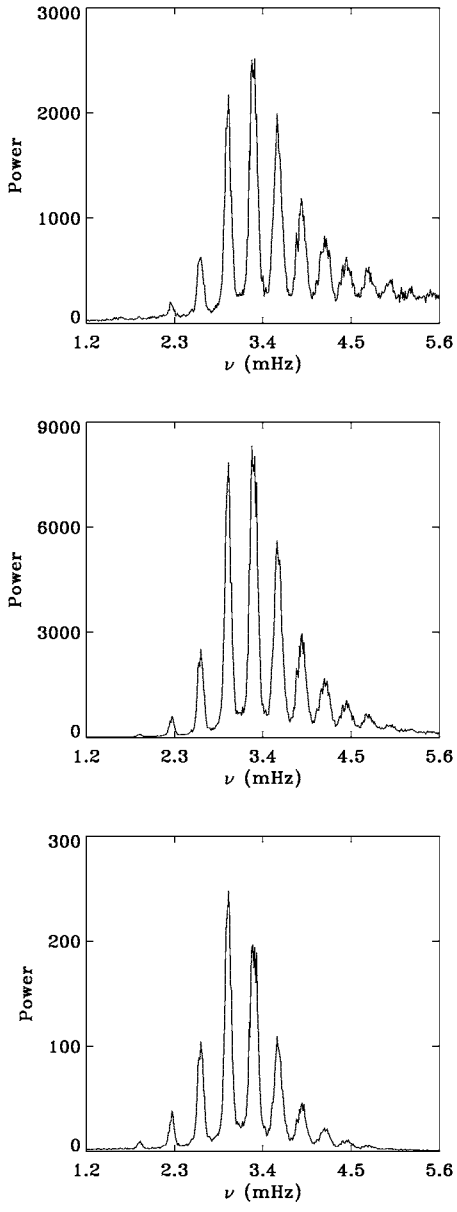

Figure 1. Power spectra obtained from (bottom) GONG Ni, (middle) MOTH K, and (top) MOTH Na line images at the disk center for ℓ = 337. The maximum power is obtained for the K line and the minimum for the Ni line.

Each region covers 128 × 128 pixels and was remapped and tracked for 1440 min. The sample m-averaged power spectra for all three lines are shown in Figure 1. In order to study the variation in mode characetristics with the observing height, we compare regions at the same location.

3. COMPARISON OF MODE PARAMETERS

In our analysis, we first consider the MOTH data sets for the Na and K lines, the GONG data sets for the Ni line, and the separate MWO Na data set. We determine the mode parameters for each region by fitting Equations (1) and (2) for all three spectral lines and examining the variation in parameters. Figure 2 shows the comparison of modes obtained with the Ni, K and Na lines at disk center using Equation 1. It is clearly seen that most of the modes for $0 \leq n \leq 6$ are fitted in all three cases in the range ℓ = 100 - 600, thus providing a sufficient number of common modes for the comparison. We have analyzed the properties of the oscillation modes, namely, frequency, amplitude, line width, background power and asymmetry.

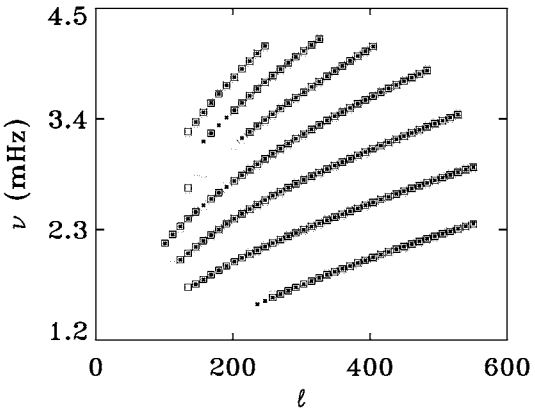

Figure 2. Comparison between the set of modes obtained with the Ni line (blue stars), the K line (red squares) and the Na line (green circles) at the disk center.

3.1. Mode frequencies

It is expected that the frequencies are independent of the type of observable and the spectral line used to obtain the observations. To test this, we compare frequencies obtained using the three different lines. In Figure 3, we show the difference in frequencies computed from the K data with respect to those obtained from Ni as a function of frequency at the disk center. We show the difference for frequencies obtained using the symmetric profile (Figure 3a), and the asymmetric profile (Figure 3b) models. The non-zero values of the frequency difference indicate different values of the frequencies obtained for the same period but for different spectral lines. We notice that the frequencies for K and Ni lines have resonable agreement with each other within an uncertainity of 1σ for the symmetric profile models, however the difference

© European Space Agency • Provided by the NASA Astrophysics Data System

2006ESASP.624E.103J

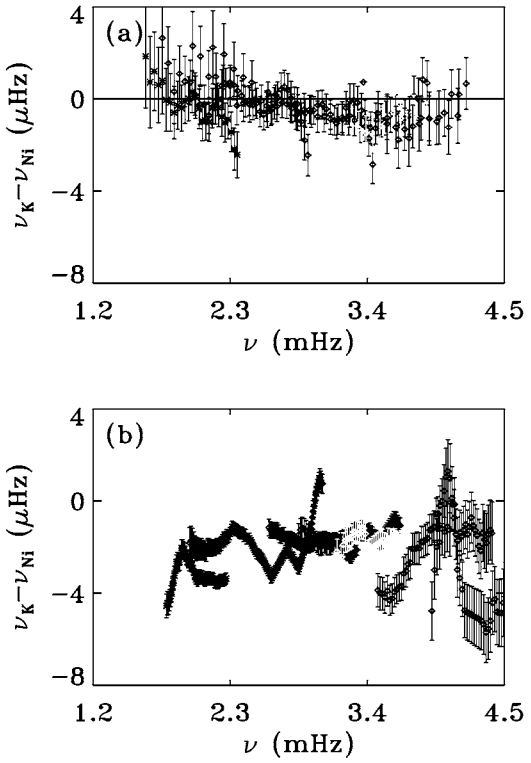

Figure 3. The frequency dependence of the difference in frequencies obtained with the K and Ni data using (a) symmetric and (b) asymmetric peak profile models. Stars (black) are for f modes and diamonds are for p modes. Different colors indicate different n ridges in the ℓ - ν diagram.

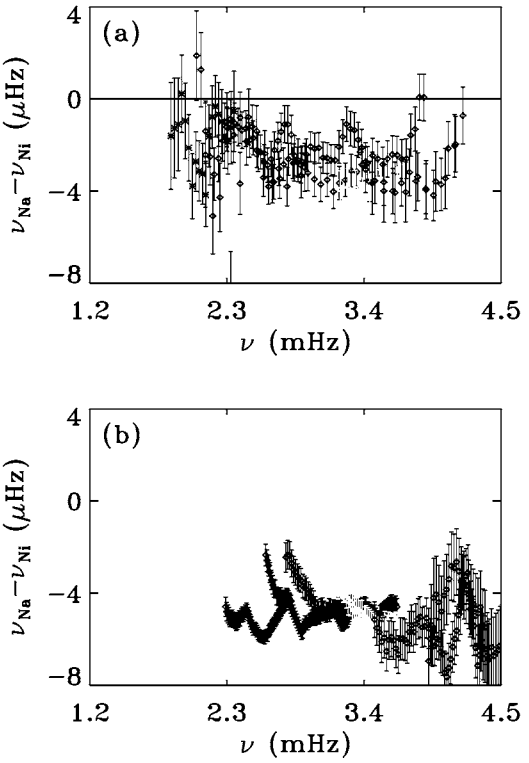

Figure 4. Similar to Fig 3 but for the difference in frequencies obtained with the Na and the Ni line data. It is seen that the modes for n = 0 were not fitted in the asymmetric profile mode.

is much larger if the peaks are considered to be asymmetric. The frequency difference between Na and the Ni lines is shown in Figure 4. In this case, we find a difference for both symmetric and asymmetric models. The n = 0 modes were not fitted in the asymmetric model.

In an earlier work, Rhodes et al. [9] compared frequencies of high-ℓ and high-frequency global modes computed from time series of Na and Ni lines. While they did not find any significant difference between these frequencies, the differences found in their work is of the same order as we obtain in our analysis of a small region. Since the temporal frequency resolution is inversely proportional to the length of the time series, longer time series provide more reliable estimates of the frequencies. Our technique tracks a region for more than 24 h and MWO datasets cover a period of about eight hours in a day. Therefore, errors in the MWO frequencies in our analysis are largerf than those for the GONG and MOTH data. Figure 5 shows the difference in frequencies obtained for MWO Na and GONG Ni data sets by tracking the center region for 450 min. It is clearly seen that the errors are larger compared to Figure 4, however the estimated difference in frequencies is generally within 1σ. In Figure 6, we show the difference between the two sets of frequencies obtained with the Na line. It is surprising that the difference is not approximately zero, since both the MWO and MOTH instruments use magneto-optical filters. The cause of this difference is currently under investigation.

To eliminate possible systematic errors due to different observing conditions, we calculate the change in frequencies between two locations on the solar disk with the same spectral line. It is shown by Hindman et al. [16] that there are local frequency shifts in various regions on the solar disk which are well correlated with the corresponding magnetic activity. Therefore, if magnetic activity does not contaminate the observations via changes in the spectral line shape, the change in frequencies between two locations should be same for all three spectral lines. We display these local changes in frequencies at two different locations on the equator.

All frequency shifts are calculated with reference to the center region using symmetric and asymmetric profile models. Figure 7 shows frequency shifts for 30°E at the equator. We find a scatter in the local shift with the symmetric model, while there is a strong frequency dependence in the asymmetric model shifts. The reason for this difference is beyond the scope of this paper. Here, we are only interested in relative shifts for all three lines which are consistent in both cases. Better agreement is obtained at higher frequencies. In Figure 8, we plot frequency shifts for 30°W at the equator. It is clear that the shifts in frequencies between two locations within the same spectral line are in reasonable agreement with

© European Space Agency • Provided by the NASA Astrophysics Data System

2006ESASP.624E.103J

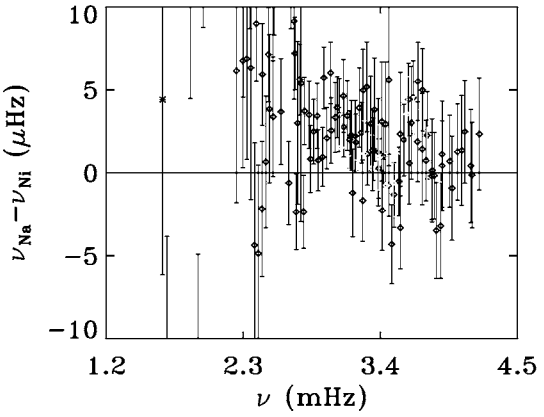

Figure 5. Difference between Ni (GONG) and Na (MWO) frequencies. The frequencies are calculated by tracking the a region at the disk center for 450 min. Different colors are for different n values.

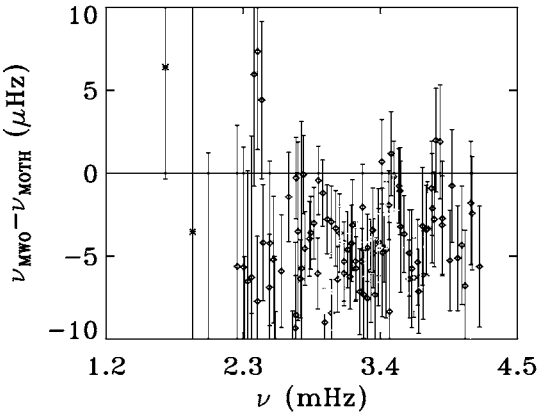

Figure 6. Same as Figure 5 but the difference is between the frequencies obtained from the MOTH and MWO sodium line observations.

those obtained for the other lines. This suggests that magnetically-induced spectral line changes do not affect the frequency determination, but a more thorough analysis that quantifies the activity level remains to be done.

3.2. Mode Amplitude

Observations of different spectral lines probe different altitudes in the solar atmosphere. Salabert et al. [17] have compared mode amplitudes for the low-degree global modes obtained in K(IRIS network) and Na (MARK-I and LOWL observations). They found that the amplitude for the Na line is higher than that obtained for the K line. These findings are consistent with the generally accepted idea that the oscillation amplitude increases with altitude because of the strong decrease of density with altitude in the solar atmosphere.

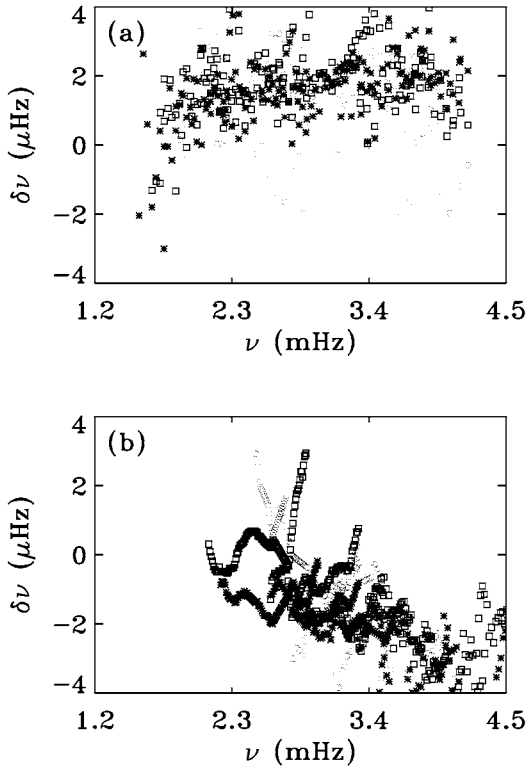

Figure 7. Comparison between the change in frequency at 30°E with reference to the disk center for Ni line (blue stars), the K line (red squares) and the MOTH Na line (green circles) at the disk center using (a) symmetric, and (b) asymmetric peak profile models. Errors are not plotted for the sake of clarity. The estimated errors are of the same order as in Figures 3 and 4.

In order to compare amplitudes for the high-degree modes, we plot the variation in mode amplitude as a function of frequency for all three spectral lines in Figure 9. The maximum amplitude is found for the K line and the minimum for the Ni line. Since the Ni line is formed in the lower photosphere and the K and Na are in upper photosphere and lower chromosphere respectively, we expect the maximum amplitude for the Na line. Instead, the maximum amplitude is seen with the K line, in contrast to the results for the low-degree global modes [17]. The comparison of power spectra shown in Figure 1 also indicates that the maximum power is in the peaks of the K line observatons.

We note that the amplitude obtained for the Na line is lower than in the Ni line for low-frequency $n = 0$ modes. Rhodes et al. [9] also found lower power densities for MWO Na compared to MDI Ni for low-n ridges ($n \leq 3$) where they show the frequency dependence of the ratio of the power densities. Their analysis is based on global modes but covers a larger range of frequency. Is there similar behavior for the local modes? For higher n modes ($n \geq 2$), the amplitude observed in the K and Na lines does converge at high frequencies. However, we could not fit a sufficient number of modes beyond the crossing point to clearly study the behavior. We did not find any

© European Space Agency • Provided by the NASA Astrophysics Data System

2006ESASP.624E.103J

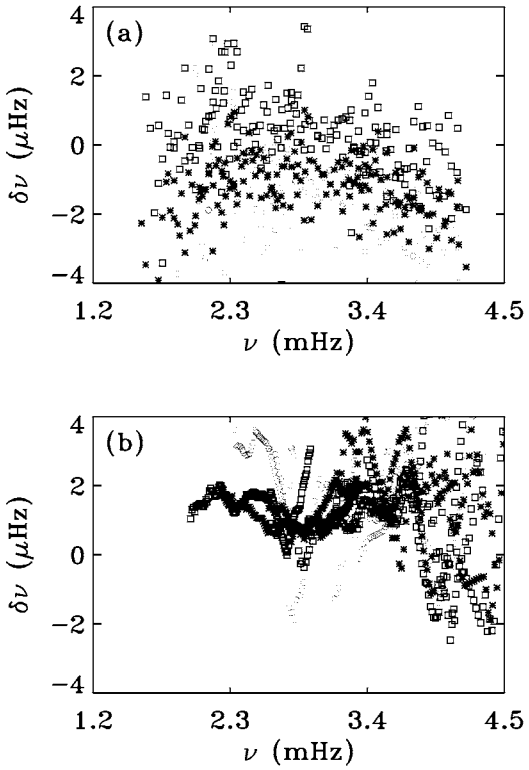

Figure 8. Similar to Figure 7 but at 30°W at the equator.

change in the behavior between the symmetric and asymmetric peak profile models.

We have also studied the variation in mode width and the background power with observing height. The width of the peak is a measure of the life time of the modes and the detection of the modes depends on the signal-to-noise ratio. We show the variation in width and background in Figures 10 and 11. We do not see any significant difference in the mode width, indicating that the apparent life times are independent of the observing height. A similar conclusion was made by Basu, Antia & Bogart [8] using three different observables. The asymmetry in the peaks, represented by the parameter S in Equation 2, is shown in Figure 12. In all three cases, S is negative except for a very few exceptions, in agreement with earlier observations.

4. SUMMARY

Our major findings are summarized below:

1. There are differences in mode frequencies obtained with different spectral lines. The frequencies obtained with Ni and K using a symmetric profile model agree to within 1σ.

2. The change in frequency obtained from different locations on the solar disk for the same spectral line is independent of the line.

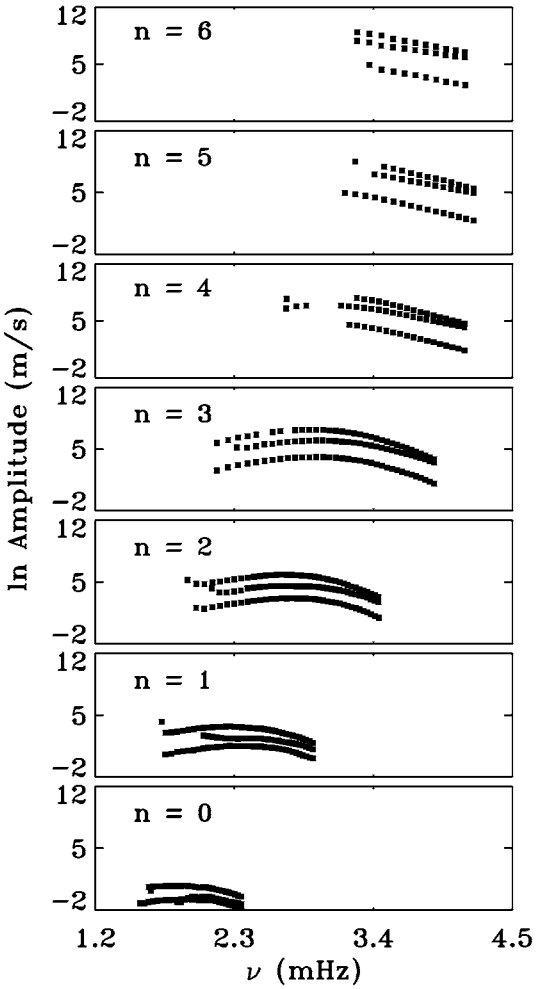

Figure 9. Mode amplitude at the disk center as a function of frequency for different spectral lines. Each panel has three curves; the lower curve is for the Ni line (blue), middle for the Na line (green) and the upper for the K line (red).

3. The mode amplitude obtained with K and Na lines are higher than those obtained with the Ni line. However, modes obtained with the K line have higher amplitude than Na, opposite to what is expected from solar models i.e. the mode amplitude should increase with increasing height and decreasing density. On the other hand, if the modes are evanescent, there will be an exponential decrease in the amplitude of the modes, which will compete with decreasing density. A thorough investigation is required to understand the variation in the mode amplitude with observing height.

4. There is no significant change in the line width, implying that the life times of the modes are independent of the height of formation of the spectral line used to observe the oscillations. All differences are within 1σ. We also did not find any apparent change in the asymmetry of the peaks.

© European Space Agency • Provided by the NASA Astrophysics Data System

2006ESASP.624E.103J

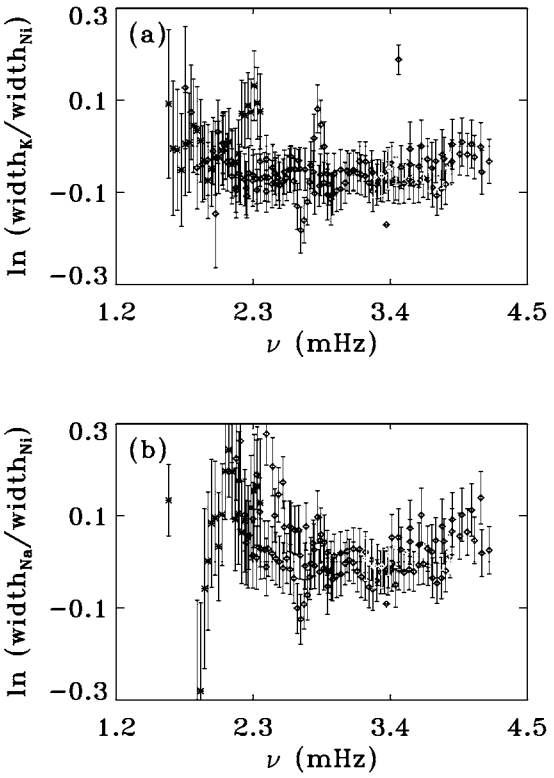

Figure 10. Comparison of the line width of modes obtained from different spectral lines. The logarithm of the ratio of the width for (a) K and Ni, and (b) and Na and Ni are plotted. Different colors indicate different n values.

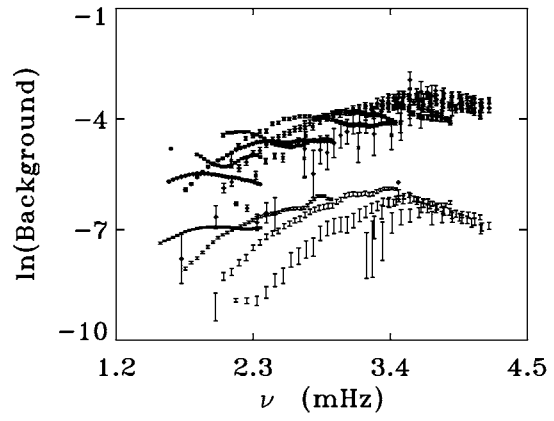

Figure 11. Comparison of background power for different spectral lines: Ni (lower curve, blue), K (red), and Na (green) lines.

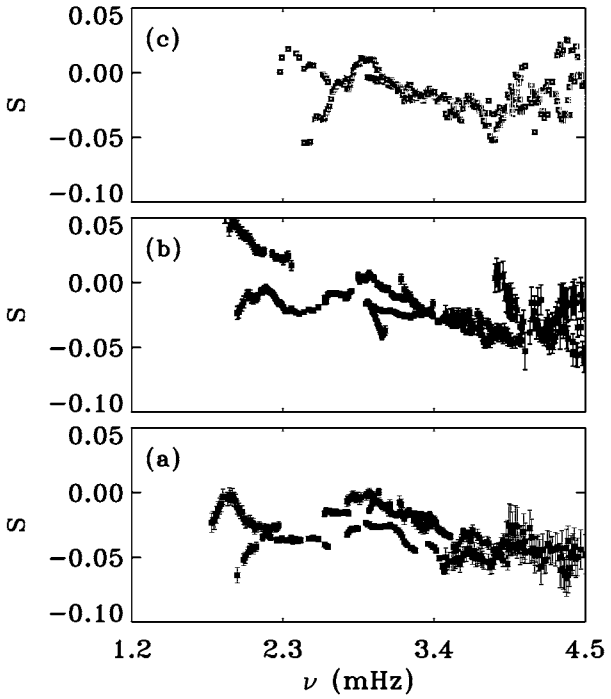

Figure 12. The asymmetry parameter, S, obtained from fitting (a) Ni, (b) K, and (c) Na lines power spectra.

5. The background power in modes varies with observing height. The minimun power was obtained by fitting the Ni line data.

ACKNOWLEDGEMENTS

Many useful discussions with Irene González-Hernández are gratefully acknowleged. This work utilizes data obtained by the Global Oscillation Network Group (GONG) program, managed by the National Solar Observatory, which is operated by AURA, Inc. under a cooperative agreement with the National Science Foundation. The data were acquired by instruments operated by the Big Bear Solar Observatory, High Altitude Observatory, Learmonth Solar Observatory, Udaipur Solar Observatory, Instituto de Astrofísica de Canarias, and Cerro Tololo Interamerican Observatory. It also utilizes data obtained at South Pole Station funded by National Science Foundation (Office of Polar Programs) and Mt. Wilson 60 Foot Tower.

REFERENCES

[1] Komm, R., Howe, R. & Hill, F., 2000, ApJ 543, 1272

[2] Jain, K. & Bhatnagar, A., 2003, Solar Phys. 213, 257

[3] Howe, R. Chaplin, W. J., Elsworth, Y. Hill, F.,Komm, R., Isaak, G.R. & New, R., 2006, MNRAS 369, 933

© European Space Agency • Provided by the NASA Astrophysics Data System

2006ESASP.624E.103J

[4] Tripathy, S. C., Hill, F., Jain, K. & Leibacher, J., 2006, these proceedings

[5] Reiter, J., Rhodes, Jr., E. J., Kosovichev, A. G. & Schou, J., 2004, in SOHO14/GONG2004, Helio- and Asteroseismology: Towards a Golden Future, ed. D. Danesy (ESA SP-559, Noordwijk:ESA), 61

[6] Rajaguru, P., Basu, S.& Antia, H. M., 2001, ApJ 563, 410

[7] Howe, R., Komm,R.W., Hill, F., Haber, D.A. & Hindman, B.W., 2004, ApJ 608, 562

[8] Basu, S., Antia, H.M. & Bogart, R.S., 2000, in SOHO10/GONG2000, Helio- and Asteroseismology at the Dawn of the Millennium, (ESA SP-464, Noordwijk:ESA), 183

[9] Rhodes, Jr., E. J., Reiter, J., Kosovichev, A. G., Schou, J., Scherrer, P.H., Rose, P.J., Irish, S. & Jones, A. R., 1998, in SOHO6/GONG98, Structure and Dynamics of the Interior of the Sun and Sun-like Stars, ed. S.G. Korzennik and A. Wilson (ESA SP-418, Noordwijk:ESA), 311

[10] Hill, F., Stark, P. B., Stebbins, R. T., Anderson, E. R., Antia, H. M., Brown, T. M., Duvall, T. L., Jr., Haber, D. A., Harvey, J. W., Hathaway, D. H., Howe, R., Hubbard, R., Jones, H. P., Kennedy, J. R., Korzennik, S. G., Kosovichev, A. G.; Leibacher, J. W. et al., 1996, Science, 272, 1292

[11] Finsterle, W., Jefferries, S. M., Cacciani, A., Rapex, P., Giebink, C., Knox, A. & Dimartino, V, 2004, Solar Phys. 220, 317

[12] Hill, F., 1988, ApJ 333, 996

[13] Haber, D., Hindman, B.W., Toomre, J., Bogart, R.S., Larsen, R.M. & Hill, F., 2002, ApJ 570, 885

[14] Basu, S.& Antia, H. M., 1999, ApJ 525, 517

[15] Nigam, R. & Kosovichev, A.G., 1998, ApJ 505, L51

[16] Hindman, B.W., Haber, D.,Toomre & Hill, F., 2000, Sol Phys. 192, 363

[17] Salabert, D., Fossat, E., Gelley, B. Tomczyk, S. et al., 2002, A&A 390, 717

© European Space Agency • Provided by the NASA Astrophysics Data System